

Research Article

Investigating Effect of Road Roughness and Vehicle Speed on the Dynamic Response of the seven degrees-of-freedom Vehicle Model by using Artificial Road Profile

O. P. Joshi^{†*}, T. A. Jadhav[†], P. R. Pawar[‡] and M. R. Saraf[‡]

[†]Sinhgad College of Engineering, Department of Mechanical Engineering, Savitribai Phule Pune University, Vadgaon, Pune, India - 411 041

[‡]The Automotive Research Association of India, Structural Dynamics Laboratory, Kothrud, Pune, India- 411 004

Accepted 20 July 2015, Available online 27 July 2015, Vol.5, No.4 (Aug 2015)

Abstract

Ride-comfort and durability of the vehicle are influenced by irregularities on the road surface and varying vehicle speed due to road traffic conditions. Hence it becomes important to analyze the effect of road roughness on vehicle vibration response. In this work, effect of road roughness and vehicle speed on the dynamic response of a Sport Utility Vehicle (SUV) is investigated through vehicle simulation. The vehicle model used is the seven degrees-of-freedom full car vertical dynamic ride model. Features of the model include suspension characteristics for each of the four tires, and vehicle body. The simulation of the seven degrees-of-freedom state space model is carried out using MATLAB. Particularly, the response of the seven degrees-of-freedom model is analyzed for ride-comfort on four different artificial road profiles simulated using Gaussian Moving Average (GMA) as per ISO 8608 and at three different vehicle speeds. It is observed that road roughness and vehicle speed have a significant impact on the ride-comfort and load history.

Keywords: Artificial road profile, Seven degrees-of-freedom vehicle model, Load, Ride-comfort, Vehicle simulation

1. Introduction

Dynamic response of the vehicle (i.e. vehicle vibration) is influenced by road profile excitation, as road and pavements are responsible for transient displacement excitations to which vehicles are exposed during an operation at a prevailing traffic speed. Prevailing speed mentioned is constrained by traffic conditions, road conditions, and local regulation about the vehicle speed. Hence, interest of vehicle dynamics engineers is always focused on a road roughness and vehicle vibration in the frequency range of interest, which corresponds to a wave number range appropriate to prevailing traffic speed.

Several researchers have attempted to analyze the effect of various operating and system parameters on the dynamic behavior of the vehicle. P. Pawar, *et al.* (2009) have investigated the effects of road roughness on a vehicle's ride-comfort and durability by the experimental data acquisition method. They observed that, as International Roughness Index (IRI) of a road surface increase, the standard deviation of axle and chassis acceleration and suspension displacement increases. Road profiling provides an opportunity to segregate small patches of rough terrain out of total

stretch, which are important from vehicle durability point of view. P. Johannesson, *et al.* (2012, 2014) have studied the reconstruction of the measured road profile using stochastic road profile models. For reconstruction of road profile, road roughness indicator like IRI was taken from the measurement of road profile information. They concluded that road profile can be reconstructed efficiently from condensed roughness data in the form of IRI values or roughness coefficients. K. Bogsjo, *et al.* (2002) have studied the statistical description and analysis of road surface irregularities. Mathematical road models viz. Laplace Moving Average, Non-homogenous Gaussian, Homogeneous Gaussian, Gaussian Moving Average are proposed and verified with Swedish road roughness data of 230 km. The importance of the road section with a high degree of road roughness in a fatigue life calculation has been highlighted. R. Ma, *et al.* (2013) have discussed the state of art in the road profile characterization. Various road characterization methods viz. PSD, Auto regression, Markov chain, Wavelet Transform, Hilbert-Huang Transformation are reviewed. They concluded that, vehicle design and development time could be cut down by making use of proper road profile characterization technique to predict chassis loads and the vehicle response. L. Munari, *et al.* (2012) have discussed method for

*Corresponding author: O. P. Joshi

retrieving road profile from a given Power Spectral Density (PSD) for ride simulation. It is been concluded that road profiles are necessary for design of vehicle and its accessories for ride-comfort and durability. M. Soliman, et al. (2013) have investigated the effect of road roughness on the ride-comfort by using a half car vehicle model simulation with given fixed configuration.

Considering work done in the past, there is a scope to study the effect of operating parameters on dynamic response of the vehicle by using the more accurate vehicle and road model. In this work, the effect of road roughness and vehicle speed on the response of typical Sports Utility Vehicle (SUV) is investigated. The vehicle model used for investigation is a state space seven degrees-of-freedom full car model vertical dynamic ride model. The model derived is capable of predicting time history for axle accelerations, Centre of Gravity (CG) acceleration, wheel loads, spring loads, and damper loads. Response of the seven degrees-of-freedom vehicle model with typical SUV configuration is analyzed for ISO 8608 [8] class A, B, C, and D road profile. Gaussian Moving Average (GMA) model is used to retrieve artificial road profile from ISO 8608 PSD. To investigate effect of the vehicle speed on the vehicle response, vehicle speed range of 10 to 45 km/h is considered. To investigate effects of road roughness and vehicle speed variation on vehicle response minimum, maximum and Root Mean Square (RMS) values of vehicle body CG acceleration, suspension spring and axle loads are compared. Simulation of the seven degrees-of-freedom state space model and the artificial road profile creation is carried out using MATLAB. This paper is organized in the following sequence - vehicle model, artificial road model, finally, the MATLAB simulation results are discussed followed by conclusion.

2. Vehicle Model

Mathematical modeling of a vehicle as vibrating system is widely used to study the vehicle response to given bump or pothole road profile. The vehicle can be mathematically modeled in order of their increasing complexity as quarter car, half car, and full car respectively, as per analysis requirements. M. Mahala et al (2009) have concluded that the seven degrees-of-freedom vehicle model should be used for accurate prediction of vehicle response to given road profile. In this work, seven degrees-of-freedom vehicle model is used.

2.1 Vehicle Model Description

Seven degrees-of-freedom mathematical model is derived to study the influence of the road roughness and vehicle speed on the typical SUV ride-comfort and durability loads. The seven degrees-of-freedom of the vehicle model are the heave Z_{cg} , pitch θ , roll Φ of the vehicle body, and the vertical displacements (Z_{rl1} , Z_{rr1} ,

Z_{rl2} , Z_{rr2}) of each of the four un-sprung masses (M_{wl1} , M_{wr1} , M_{wl2} , M_{wr2}). All of the displacements mentioned above are absolute quantities. The sprung mass and un-sprung mass is modeled as a rigid body.

The vehicle model consists of suspended masses, which are coupled by parallel linear springs and viscous dampers as shown in Figure 1. The inputs are transmitted from the road to the vehicle body via tires, which are represented as equivalent linear spring and viscous damping, and "suspensions" which approximate stiffness and damping characteristics. The tires are connected to the vehicle body (chassis) by another equivalent linear spring and damper, which approximate the vehicle axle suspension elements. The driver is modeled as a lumped mass connected to vehicle body via another linear spring and viscous damper which approximate seat cushioning.

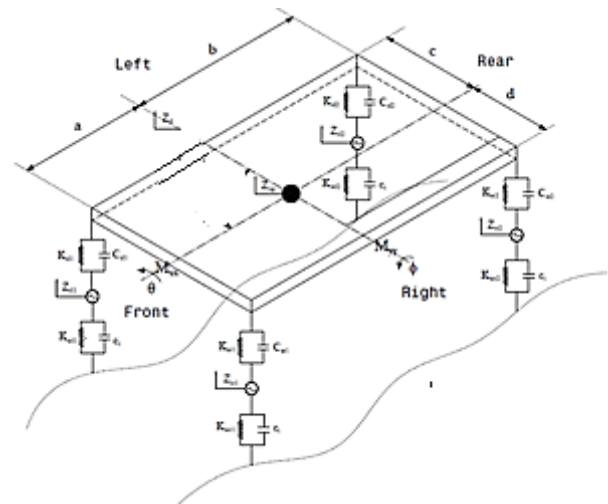


Fig.1 Seven degrees-of-freedom model

The equations of motion for the seven degrees-of-freedom vehicle model are derived using Newton's second law of motion and free body diagram concept. The full derivation is as given below from Equations (1) to (7).

For vehicle bounce, motion (Sprung mass):

$$M_s \ddot{Z}_{cg} = -K_{sr1}(Z_{cg} - \theta a - \phi c - Z_{wr1}) - K_{sl1}(Z_{cg} - \theta a + \phi d - Z_{wl1}) - K_{sr2}(Z_{cg} + \theta b - \phi c - Z_{wr2}) - K_{sl2}(Z_{cg} + \theta b + \phi d - Z_{wl2}) - C_{sr1}(\dot{Z}_{cg} - \dot{\theta} a - \dot{\phi} c - \dot{Z}_{wl2}) - C_{sl1}(\dot{Z}_{cg} - \dot{\theta} a + \dot{\phi} d - \dot{Z}_{wl2}) - C_{sr2}(\dot{Z}_{cg} + \dot{\theta} b - \dot{\phi} c - \dot{Z}_{wl2}) - C_{sl2}(\dot{Z}_{cg} + \dot{\theta} b + \dot{\phi} d - \dot{Z}_{wl2}) \quad (1)$$

For vehicle body pitch motion:

$$I_{yy} \ddot{\theta} = K_{sr1}(Z_{cg} - \theta a - \phi c - Z_{wr1})a - K_{sl1}(Z_{cg} - \theta a + \phi d - Z_{wl1})a - K_{sr2}(Z_{cg} + \theta b - \phi c - Z_{wr2})b - K_{sl2}(Z_{cg} + \theta b + \phi d - Z_{wl2})b - C_{sr1}(\dot{Z}_{cg} - \dot{\theta} a - \dot{\phi} c - \dot{Z}_{wr1})a + C_{sl1}(\dot{Z}_{cg} - \dot{\theta} a + \dot{\phi} d - \dot{Z}_{wl1})a - C_{sr2}(\dot{Z}_{cg} + \dot{\theta} b - \dot{\phi} c - \dot{Z}_{wr2})b - C_{sl2}(\dot{Z}_{cg} + \dot{\theta} b + \dot{\phi} d - \dot{Z}_{wl2})b \quad (2)$$

For vehicle body roll motion:

$$I_{xx}\ddot{\phi} = K_{sr1}(Z_{cg} - \theta a - \phi c - Z_{wr1})c - K_{sl1}(Z_{cg} - \theta a + \phi d - Z_{wl1})d + K_{sr2}(Z_{cg} + \theta b - \phi c - Z_{wr2})c - K_{sl2}(Z_{cg} + \theta b + \phi d - Z_{wl2})d + C_{sr1}(\dot{Z}_{cg} - \dot{\theta}a - \dot{\phi}c - \dot{Z}_{wr1})c - C_{sl1}(\dot{Z}_{cg} - \dot{\theta}a + \dot{\phi}d - \dot{Z}_{wl1})d + C_{sr2}(\dot{Z}_{cg} + \dot{\theta}b - \dot{\phi}c - \dot{Z}_{wr2}) + C_{sl2}(\dot{Z}_{cg} + \dot{\theta}b + \dot{\phi}d - \dot{Z}_{wl2}) \quad (3)$$

For front right wheel bounce motion:

$$M_{wr1}\ddot{Z}_{wr1} = K_{sr1}(Z_{cg}) - C_{sr1}(\dot{Z}_{cg}) - K_{sr1}a(\theta) - C_{sr1}a(\dot{\theta}) - K_{sr1}c(\phi) - C_{sr1}c(\dot{\phi}) - (K_{sr1} + K_{wr1})(Z_{wr1}) - C_{sr1}(\dot{Z}_{wr1}) + K_{wr1}Z_{rr1} + C_t(Z_{rr1}) \quad (4)$$

For front left wheel bounce motion:

$$M_{wl1}\ddot{Z}_{wl1} = K_{sl1}(Z_{cg}) + C_{sl1}(\dot{Z}_{cg}) - K_{sl1}a(\theta) - C_{sl1}a(\dot{\theta}) + K_{sl1}d(\phi) + C_{sl1}d(\dot{\phi}) - (K_{sl1} + K_{wl1})(Z_{wl1}) - C_{sl1}(\dot{Z}_{wl1}) + K_{wl1}Z_{rl1} + C_t(Z_{rl1}) \quad (5)$$

For rear right wheel bounce motion:

$$M_{wr2}\ddot{Z}_{wr2} = K_{sr2}(Z_{cg}) + C_{sr2}(\dot{Z}_{cg}) + K_{sr2}b(\theta) + C_{sr2}a(\dot{\theta}) - K_{sr2}c(\phi) - C_{sr2}c(\dot{\phi}) - (K_{sr2} + K_{wr2})(Z_{wr2}) - C_{sr2}(\dot{Z}_{wr2}) + K_{wr2}Z_{rr2} + C_t(Z_{rr2}) + C_t(Z_{rr2}) \quad (6)$$

For rear left wheel bounce motion:

$$M_{wl2}\ddot{Z}_{wl2} = K_{sl2}(Z_{cg}) + C_{sl2}(\dot{Z}_{cg}) + K_{sl2}b(\theta) + C_{sl2}b(\dot{\theta}) + K_{sl2}d(\phi) + C_{sl2}d(\dot{\phi}) - (K_{sl2} + K_{wl2})(Z_{wl2}) - C_{sl2}(\dot{Z}_{wl2}) + K_{wl2}Z_{rl2} + C_t(Z_{rl2}) \quad (7)$$

3 Road Model

3.1 Classification of Road Profiles as per ISO 8608

The ISO 8608 [8, 12] has proposed a road roughness classification (Class A-H) based on the PSD as shown in Figure 2. In the ISO 8608 classification, the relationships between the PSD and spatial frequency for different classes of road roughness are approximated by single straight lines with single slopes on log-log scale, as shown in Figure 2. The ISO 8608 standard uses a fixed waviness (slope) for road profile PSD as N= 2. The relationships are as given below in equation (9).

Hence, PSD function becomes,

$$S(\Omega) = S(\Omega_0) (\Omega/\Omega_0)^{-2}, \quad (2\pi/90 \text{ rad/m} \leq \Omega \leq 2\pi/0.35 \text{ rad/m}) \quad (8)$$

As per ISO Class A road is considered as a good quality of road profile with road roughness coefficient less than 2×10^{-6} (m²/rad/m), whereas class H road considered as the worst quality road with road roughness coefficient greater than 8192×10^{-6} (m²/rad/m)

3.2 Gaussian Moving Average Parallel Road Model

Gaussian Moving Average road profile model, is used to retrieve artificial road profile from ISO 8608 road roughness spectrum. It is a moving average of white noise. Mathematically moving average is convolution of a kernel function $g(x)$ with an infinitesimally 'white noise' process having variance equal to spatial discretization step dx .

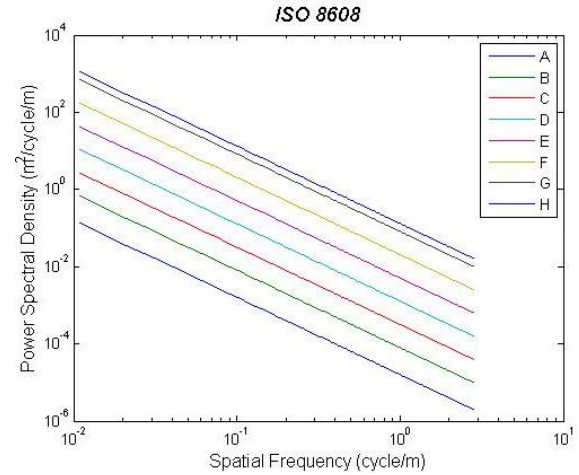


Fig. 2 Classification of road roughness as per ISO 8608

3.2.1 Model Description

Consider $g(x)$, as kernel function, which is normalized so that its square integrates to one

Standardized GMA with mean zero and variance one

$$Z(x) = \int g(x - u)Z_i \sqrt{dx} \quad (9)$$

Where,

Z_i =Independent standard Gaussian random variables, while dx is the discretization step.

The kernel $g(x)$ defined by its Fourier Transform viz.

$$(Fg)(\Omega) = \sqrt{2\pi S(\Omega)} \quad (10)$$

Where F stands for Fourier transform.

In order to generate correlated right $Z_R(x)$ and left $Z_L(x)$ road profile normalized cross spectrum $K(\Omega)$ is defined as,

$$K(\Omega) = \exp(-f|\Omega|) \quad (11)$$

Where, $f=2$

By making use of the above mentioned normalized cross spectrum $K(\Omega)$, two kernel $g(x)$

$$(F\tilde{g}_1)(\Omega) = \frac{(\sqrt{(1+K)} + \sqrt{(1-K)})}{2} \quad (12)$$

$$(F\tilde{g}_2)(\Omega) = \frac{(\sqrt{(1+K)} - \sqrt{(1-K)})}{2} \quad (13)$$

These calculated kernels \tilde{g}_1 and \tilde{g}_2 are used to introduce correlation between left and right road profiles. The kernel $g(x)$ defined earlier in the will be used to get the desired PSD. Now define two kernels $g_1(x)$ and $g_2(x)$ by

$$Fg_1(\Omega) = (Fg)(\Omega) \cdot (F\tilde{g}_1)(\Omega) \tag{14}$$

$$Fg_2(\Omega) = (Fg)(\Omega) \cdot (F\tilde{g}_1)(\Omega) \tag{15}$$

Gaussian process having spectrum $S(\Omega)$ and coherence $|K(\Omega)|^2$ are given by the Gaussian Moving Averages,

$$Z_L(x) = (\sum g_1(x - x_i)Z_{1i} + \sum g_2(x - x_i)Z_{2i})dx \tag{16}$$

$$Z_R(x) = (\sum g_2(x - x_i)Z_{1i} + \sum g_1(x - x_i)Z_{2i})dx \tag{17}$$

Where, Z_{1i} and Z_{2i} are independent standard Gaussian random variables and with equality in dx limit as dx tends to zero.

4. Results

4.1 Verification of the seven degrees of freedom model

Validation of the MATLAB seven degrees-of-freedom state space SUV model is done by comparing simulation results with MSC.ADAMS Car simulation results.

Sin bump of 0.1 m amplitude and 8 m wavelength is created in MATLAB as well as in MSC.ADAMS CAR. Road builder functionality is used to create the road Sin bump in MSC.ADAMS Car. Mass, suspension and tire properties are assigned to multibody model in MSC.ADAMS Car are same as that of used for simulating the seven degrees-of-freedom MATLAB model.

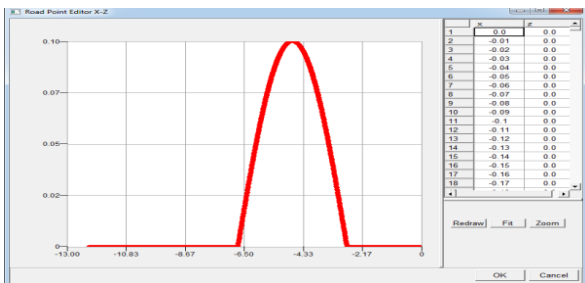


Fig. 3 Sin bump in MSC.ADAMS Car

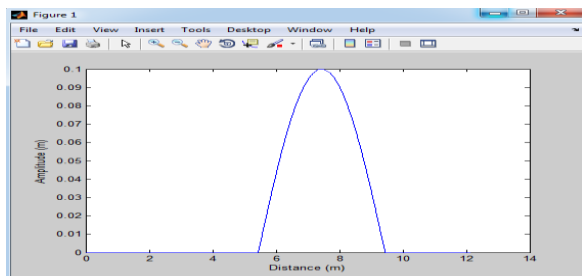


Fig. 4 Sin bump in MATLAB

Figure 3 shows the Sin bump road profile MSC.ADAMS Car while Figure 4 shows the Sin bump generated in the MATLAB. Both the simulations are carried out for vehicle speed of 10 kmph and sample rate of the 100 Hz.

Time history results obtained for various dynamic response like body Center of Gravity (CG) displacement, CG acceleration, body pitch angle, front axle acceleration through MATLAB and MSC.ADAMS Car simulation are compared in Figure 5.

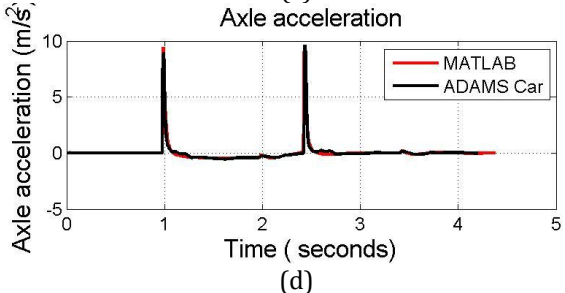
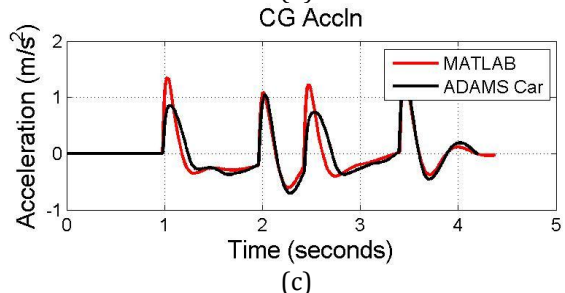
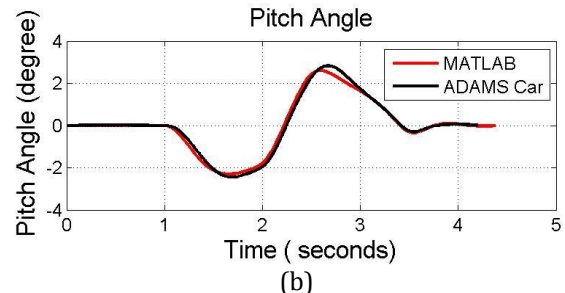
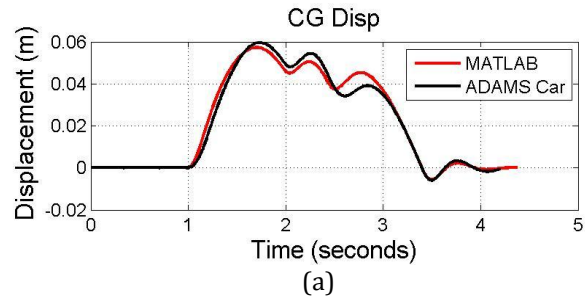


Fig. 5 Comparison between MSC.ADAMS Car and MATLAB Simulation results
(a) CG displacement (b) Pitch Angle (c) CG Acceleration (d) Axle acceleration

4.2 Road Profile Simulation

Four artificial road profiles are generated with different road roughness coefficients through MATLAB simulation. Figures 6 (a) to 6 (d) show the artificial road profile of class A, B, C, and D with road roughness

coefficients as $1 \times 10^{-6} \text{ m}^3/\text{rad}$, $4 \times 10^{-6} \text{ m}^3/\text{rad}$, $16 \times 10^{-6} \text{ m}^3/\text{rad}$, and $64 \times 10^{-6} \text{ m}^3/\text{rad}$ respectively. The length of simulated road profile is 25 m with 0.01 m discretization. After comparing Figure 6 (a) to 6 (d), it is observed that as the road roughness increases elevation of road profile also increases.

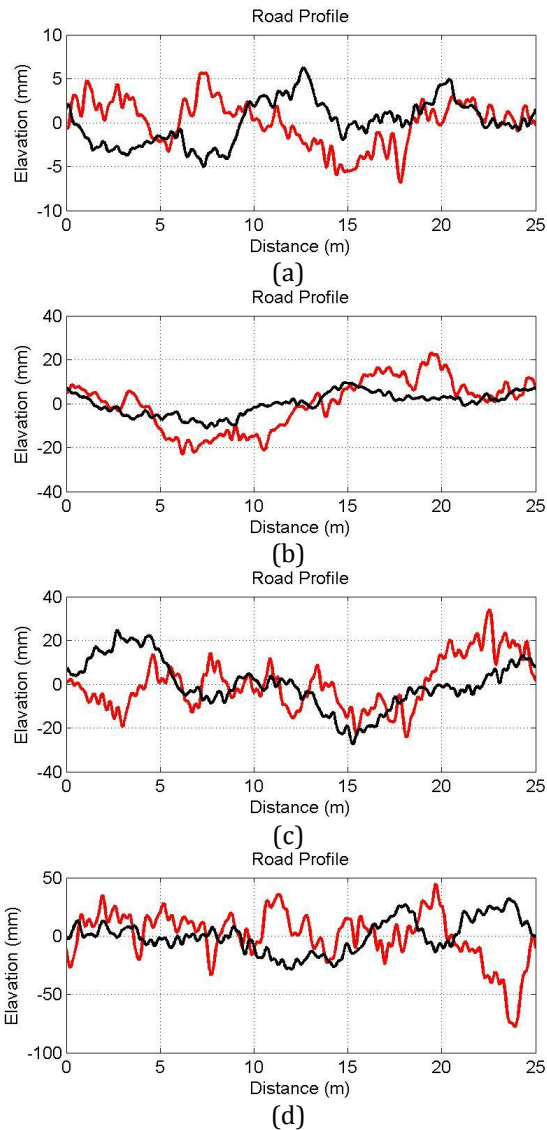


Fig. 6 Simulated road profile as per ISO 8608 spectrum by using Gaussian Moving Average Method. (a) Class A (b) Class B (c) Class C (d) Class D (Red-Left side road profile, Black- Right side road profile)

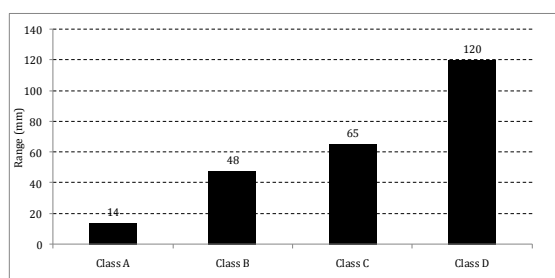


Fig. 7 Road elevation comparison four different class of the simulated road

Figure 7 shows the range of elevation for all classes of simulated road profiles.

4.3 Investigation on the Effect of Road Roughness on the Dynamic Response of the Vehicle

In order to investigate effect of road roughness on dynamic vehicle vibration response, artificial road profiles generated those are mentioned in section 4.2 are used as an input to the eight degrees-of-freedom model. Dynamic response is compared for class A, class B, class C, and class D with road roughness coefficients as $1 \times 10^{-6} \text{ m}^3/\text{rad}$, $4 \times 10^{-6} \text{ m}^3/\text{rad}$, $16 \times 10^{-6} \text{ m}^3/\text{rad}$, and $64 \times 10^{-6} \text{ m}^3/\text{rad}$ respectively. Values of vehicle parameters used for simulation are given in the Appendix A.

Effect of road roughness on RMS values of CG acceleration, suspension force, and wheel load at vehicle speed of 10 km/h are shown in Table 1. It is observed that as the road roughness increases, from class A to D values for all quantities representing dynamic response viz. vehicle body CG acceleration, axle acceleration, tire dynamic load, and spring force also increase. For example, RMS value of the spring force is lowest in class for class A road 56.41 N, whereas 131.19 N, 235.9 N, 582.87 N for class B, C, D roads respectively. The conclusion of the analysis is that road roughness information is important for evaluation of dynamic response of vehicle.

Table 1 Effect of road roughness on the dynamic response of SUV (at 10km/h)

Parameter	Class A	Class B	Class C	Class D
RMS CG accln (m/s^2)	0.1	0.2	0.4	0.9
RMS Front left axle accln (m/s^2)	0.2	0.5	0.9	1.7
RMS front left tire force (N)	83.5	191.7	357.5	824.0
RMS front left spring Force (N)	56.4	131.2	235.9	582.8

4.4 Investigation on the Effect of Vehicle Speed on the Dynamic Response of the Vehicle

In order to investigate the effect of vehicle speed on dynamic response of SUV, road profile mentioned in section 4.2 are used as input to the eight degrees-of-freedom model. Simulation is carried out at three different vehicle speeds, i.e. 10 km/h, 20 km/h, and 45 km/h. After analyzing the time history response of the vehicle dynamic quantity, the results obtained for class A roads under different vehicle speeds are tabulated in the Table 2.

Table 2 Effect of vehicle speed on the dynamic response of SUV (Class A)

Parameter	10 (kmph)	20 (kmph)	45 (kmph)
RMS CG accln (m/s ²)	0.1	0.2	0.3
RMS Front left axle accln (m/s ²)	0.2	0.7	2.2
RMS front left tire force (N)	83.6	126.6	203.8
RMS front left spring Force (N)	56.4	64.0	69.7

Conclusions

Investigation on effect of road roughness and vehicle speed on dynamic response of a typical Sport Utility Vehicle (SUV) is carried out using the seven degrees-of-freedom vehicle model. Gaussian Moving Average Parallel track model is used for artificial road profile simulation as per ISO 8608 road Power Spectral Density function. It is observed that axle acceleration is the most sensitive parameter influenced by variation in vehicle speed for constant road roughness, whereas spring loads are the most sensitive parameter influenced by variation in road roughness at constant vehicle speed for give configuration of vehicle. The ride quality of vehicle deteriorates as road roughness increases. Road roughness has an impact on the durability load history as well on ride comfort. Hence, it is mandatory to have road roughness information for customer usage pattern to design a balanced configuration of the vehicle. Artificial road profile models provide an opportunity to simulate vehicle under random road profile, which resembles with actual road condition.

In future, study of vehicle vibration response and optimization of suspension parameters by using artificial road profile derived from actual road PSD could be an interesting research to work on.

References

A. M. A. Soliman, M. M. S. Kaldas, and S.A Abdallah, (2013), Influence of the road roughness on the ride and rolling resistance for passenger car, *SAE*, 2013-01-0993

P. Pawar, and M. Saraf, (2009), Measurement of road profile and study its effect on vehicle durability and ride, *SAE*, 2009-26-070.

P. Johannesson, K. Podgorski, and I. Rychlik, (2012) Modeling roughness of road profiles on parallel tracks using roughness indicators. *Int. J. Department of Mathematical Sciences, Chalmers University of Technology and Gotenborg University, ISSN 1652-9715; nr 2014:4.*

P. Johannesson, and I. Rychlik, (2012) Modeling of road profiles using roughness indicators, *Int. J. of Vehicle Design*, 2014 Vol.66, No.4, pp.317 – 346.

K. Bogsjo, K. Podgoski, and I. Rychlik, (2002) Models for Road Roughness, *Vehicle System Dynamics*, Vol. 50, No. 5, May 2002, pp. 725-747

R. Ma, H. Chemistruck, J. Ferris, (2013) State-of-the-art of terrain profile characterization models, *In. J. Vehicle Design*, Vol. 61, pp. 1-4.

L. Munari, L. Fontanella, L. Hoss, R. Marczak, (2012) Retrieving Road surface Profiles from PSDs for ride simulation of vehicles, *SAE*, 2012-36-0003.

ISO 8608 (1995), Mechanical vibration-road surface profile-reporting of measured data ISO 8608:1995, International Standard Organization, I

M. Mahala, P. Gadkari, A. Deb, (2009) Mathematical models for designings vehicles for ride comfort, *ICORD 09:Proceedings of the 2nd International Conference on Research into design*, Bangalore, India 07- 09.01.20

C. Kim, P. Ro, (2002) An accurate full ride model using model reducing techniques, *ASME Journal of Mechanical Design*, December 2002, Vol.

J. Wong, *Theory of Ground Vehicle*, John Willey & Sons, INC, 4th

Appendix A

Table A.1: Inertial and geometric dimensions of the eight degrees-of-freedom model

Sr. No.	Description	Values	Unit
1	Mass of Vehicle Body	1532	Kg
2	Mass of Front Right Wheel	45	Kg
3	Mass of Front Left Wheel	45	Kg
4	Mass of Rear Right Wheel	55.45	Kg
5	Mass of Rear Left Wheel	55.48	Kg
6	Mass of Driver	106	Kg
7	Distance from CG to Front	1.25	m
8	Distance from CG to Rear	1.47	m
9	Distance from CG to Left	0.76	m
10	Distance from CG to Right	0.76	m
11	Moment of Inertia of Body about Roll Axis	963.4	Kg-m ²
12	Moment of Inertia of Body about Pitch Axis	4719.8	Kg-m ²
13	Distance of Driver's Seat along lateral direction	0.75	m
14	Distance of Driver's Seat along longitudinal direction	0.5	m
15	Front Right Spring Stiffness	48.43	kN/m
16	Front Left Spring Stiffness	48.43	kN/m
17	Rear Right Spring Stiffness	63.75	kN/m
18	Rear Left Spring Stiffness	63.75	kN/m
19	Front Right Damping Coefficient	6000	Ns/m
20	Front Left Damping Coefficient	6000	Ns/m
21	Rear Right Damping Coefficient	4900	Ns/m
22	Rear Left Damping Coefficient	4900	Ns/m
23	Driver Seat Stiffness	3404	N/m
24	Driver Seat Damping Coefficient	1440	Ns/m

Abbreviation & Notation

ISO International Standard Organization

SUV Sports Utility Vehicle

CG Center of Gravity

PSD Power Spectral Density

IRI International Roughness Index (m/km)

FFT Fast Fourier Transformed

Z_d Displacement of Driver's Seat (m)

Z_{cg} Displacement of SUV Body CG (m)

Z_{rl1}	Displacement of Front Left (FL) Wheel (m)	K_{sl2}	Rear Left Spring Stiffness (N/m)
Z_{rr1}	Displacement of Front Right (FR) Wheel (m)	C_{wr1}	Front Right Damping Coefficient (Ns/m)
Z_{rl2}	Displacement of Rear Left (RL) Wheel (m)	C_{wl1}	Front Left Damping Coefficient (Ns/m)
Z_{rr2}	Displacement of Rear Right (RR) Wheel (m)	C_{wr2}	Rear Right Damping Coefficient (Ns/m)
θ	SUV Body Pitch Angle at CG (degree)	C_{wl1}	Rear Left Damping Coefficient (Ns/m)
Φ	SUV Body Roll Angle at CG (degree)	K_{wr1}	Front Right Tire Stiffness (N/m)
M_s	Mass of Vehicle Body (kg)	K_{wl1}	Front Left Tire Stiffness (N/m)
M_{wr1}	Mass of Front Right Wheel (kg)	K_{wr2}	Rear Right Tire Stiffness (N/m)
M_{wl1}	Mass of Front Left Wheel (kg)	K_{wl2}	Rear Left Tire Stiffness (N/m)
M_{wr2}	Mass of Rear Right Wheel (kg)	c_t	Tire Damping Coefficient (Ns/m)
M_{wl2}	Mass of Rear Left Wheel (kg)	Ω	spatial frequency (rad/m)
a	Distance from CG to Front Axle (m)	$S(\Omega)$	power spectral density function of the elevation of the road profile (m ³ /rad)
b	Distance from CG to Rear Axle (m)	N	Road Power Spectral Density Slope
c	Distance from CG to Left Wheel (m)	$g(x)$	kernel function (m ^{1/2})
d	Distance from CG to Right Wheel (m)	$Z(x)$	Road Elevation at Distance x (m)
M_{xx}	Moment of Inertia of Body about Roll Axis (kg-m ²)	Z_i	Independent standard Gaussian random variables
M_{yy}	Moment of Inertia of Body about Pitch Axis (kg-m ²)	$Z_R(x)$	Right Wheel Road Profile (m)
r_l	Distance of the seat from CG in lateral direction (m)	$Z_L(x)$	Left Wheel Road Profile (m)
r_t	Distance of the seat from CG in longitudinal direction (m)	$K(\Omega)$	Normalized Cross Spectrum
K_{sr1}	Front Right Spring Stiffness (N/m)	$g_1(x)$	Normalized Kernel
K_{sl1}	Front Left Spring Stiffness (N/m)	$g_2(x)$	Normalized Kernel
K_{sr2}	Rear Right Spring Stiffness (N/m)	Z_{1i}	Independent Standard Gaussian Random Variable
		Z_{2i}	Independent Standard Gaussian Random Variable